# A New Ionospheric Estimation Algorithm for SBAS Combining Kriging and Tomography

Juan Blanch, Todd Walter, and Per Enge. *Stanford University*

## ABSTRACT

One can divide the existing ionospheric methods for SBAS in two categories: tomography and methods relying on the thin shell model. At first sight, tomography appears to be the right choice. Tomography reconstructs the three dimensional density of the ionosphere from the available measurements. However, there are several drawbacks to tomography: the system of equations to be solved is often underdetermined – leading to artificial constraints -, the basis functions that are used are arbitrary, and the stochastic properties of the ionosphere – which are extremely variable – are not taken into account. The thin shell model methods on the other hand (including the planar fit that is currently used in the Wide Area Augmentation System (WAAS) and methods based on kriging) assume that the vertical density profile is an impulse function. This assumption is very limiting and gives rise to the vertical to slant error. But it allows us to transform a three-dimensional problem in a two dimensional estimation problem, and to easily characterize the stochastic properties of the ionosphere.

We present an ionospheric estimation method that has elements from both categories. Like tomography, it takes into account the three dimensional nature of the ionosphere, and like in the thin shell model methods mentioned (planar fit, kriging), it relies on the measured stochastic properties of the ionosphere. This method is not a heuristic mix of both methods, but rather a natural extension of kriging in three dimensions. The technique was tested using post-processed ionospheric Total Electron Content measurements from the US and Brazil.

## INTRODUCTION

The ionosphere causes the most difficult error to mitigate in Satellite Based Augmentation Systems (SBAS) [1]. This is particularly true when the ionosphere contains disturbances, which happens rarely in mid-latitudes [2] (although enough to deny service several days a year over the US [3]) and routinely in the low latitudes [4]. Currently, the ionospheric models used in SBAS rely on the thin shell approximation [5]. The error bound generated for each approximated delay is based on the correlation of the ionospheric delay projected on the thin shell [6], [7], [8]. These models work very well on quiet days over mid-latitudes and, by reducing the dimensionality, allow the augmentation system to send the ionospheric delay information to the users in a compact manner [5].

The limitations of the thin shell are well known: as the ionospheric vertical density profile departs (considerably) from the thin shell assumption, the decorrelation of the measurements deteriorates, particularly for small distances, features appear in the middle of quiet regions, and it is difficult to decide whether they are due to real ionospheric features or a particular geometry of the ray paths. To solve these problems, tomography has been proposed [9], [10]. Tomography reconstructs the electronic density in the ionosphere from the slant measurements. The user then receives a representation of the density and can reconstruct the ionospheric delay for each ray path, as well as an error bound. There are also several drawbacks to tomography: the equation to solve is underdetermined and there is no notion of decorrelation of the ionospheric density with distance; also, the basis functions used are often global, leading to the creation of artificial features at the edge of coverage, which causes large estimation errors [10].

The ionospheric estimation problem for SBAS can be separated in two sub-problems. First, we want to find the ionospheric estimation method that minimizes the estimation error (the difference between the real delay and the delay computed by a user) and that provides an error bound, assuming that the user has all the knowledge about the measurements performed at the reference stations. The second problem arises from the bandwidth limitations and the computing limitations at the receiver: the SBAS message needs to be short, and the information included needs to be processed easily; as a result, not all the measurement information can be sent to the user. (In the current SBAS standard, this problem is handled with the ionospheric grid [5].)

In this paper we will only consider the first problem: finding an estimation method that minimizes the estimation error and provides an error bound related to the geometry of the measurements and the ionospheric conditions. First, we will introduce the model used for the ionosphere. Then, we will derive the best estimation algorithm under that model. Finally, the algorithm will be evaluated in terms of the standard deviation of the estimation error and the ability to provide a reliable error bound.

## IONOSPHERIC MODEL

We would like the model to include two properties of the ionosphere: the vertical density profile (ignored in the thin shell models) and the decorrelation of the ionospheric delay as a function of distance (ignored in the tomographic models.) To this purpose, we generalize the two dimensional model that is used in kriging and is based on multivariate Gaussian random fields [7], [8] by introducing *p* layers instead of a single thin shell. As in the thin shell models, we use a local model (as opposed to global in ionospheric tomography). This allows us to assume that in each layer *k*, the vertical delay has a mean value $\varphi_k m$, where *m* is the same across the layers and $\varphi_k$ is constant and determines the mean vertical profile. We take:

$$\sum_k \varphi_k = 1 .$$

The variable *m* can interpreted as the mean vertical ionospheric delay. In each layer, the ionospheric vertical delay is:

$$I_{vertical,k} = \varphi_k \cdot \left( m + r_k\left(x\right)\right)$$

where *x* is the location of the pierce point and $r_k(x)$ is a multivariate Gaussian field with a distance dependent covariance similar to the one introduced in [findref]:

$$\operatorname{cov}\left(r_k\left(x_i\right), r_k\left(x_j\right)\right) = f\left(\left\| x_i - x_j \right\|\right) = A \exp\left(-\frac{\left\| x_i - x_j \right\|}{d}\right)$$

The random fields $r_k$ are assumed to be independent and to have the same properties in each layer. The constants are set to $A$=5 m$^2$ and $d$= 200 km. The main difference with the covariance used in kriging is the absence of the nugget effect [7] (discontinuity at the origin). There is no nugget effect because the difference between converging ray paths goes to zero (as opposed to the difference between IPP measurements as the IPPs get closer). A delay measurement is assumed to be formed as follows:

$$I_{slant,i} = \sum_{k=1}^{p} \varphi_k \cdot \left( m + r_k\left(x_{k,i}\right)\right) \cdot ob_{k,i}$$

In this equation, $x_{k,i}$ is the location of the pierce point of the i$^{th}$ measurement on the k$^{th}$ layer and $ob_{k,i}$ is the corresponding obliquity factor [5]. The purpose of this formulation is to enable the computation of a covariance between the ray paths. The layers are described in Table 1.

| Height in km | 350 | 400 | 450 | 500 | 550 | 600 | 650 |
|---|---|---|---|---|---|---|---|
| $\varphi_k$ | .25 | .125 | .125 | .125 | .125 | .125 | .125 |

***Table 1***. *Mean ionospheric vertical profile.*

Using this model we can compute the covariance between two measurements (once the mean has been removed):

$$\operatorname{cov}\left(I_{slant,i}, I_{slant,j}\right) =$$

$$E\left(\left(\sum_{k=1}^{p} \varphi_k \cdot r_k\left(x_{k,i}\right) \cdot ob_{k,i}\right)\left(\sum_{l=1}^{p} \varphi_l \cdot r_l\left(x_{l,j}\right) \cdot ob_{l,j}\right)\right)$$

$$= \sum_{k,l} \varphi_k \varphi_l ob_{k,i} ob_{l,j} \operatorname{cov}\left(r_k\left(x_{k,i}\right), r_l\left(x_{l,j}\right)\right)$$

In this paper, we have assumed that the different random fields are independent, in which case the formula is:

$$\operatorname{cov}\left(I_{slant,i}, I_{slant,j}\right) = \sum_{k=1}^{p} \varphi_k^{\,2} ob_{k,i} ob_{k,j} \operatorname{cov}\left(r_k\left(x_{k,i}\right), r_k\left(x_{k,j}\right)\right)$$

Notice that the complete covariance of the measurement includes the covariance of the measurement noise. In this paper the measurement noise covariance is noted *M*.

## ESTIMATION ALGORITHM

Almost all the ionospheric estimation techniques are linear, that is, the estimated delay for a ray path is a linear combination of the measurements (let us suppose that there are *n*) taken at the reference stations:

$$\hat{I}_{unknown} = \sum_{i=1}^{n} \lambda_i \tilde{I}_{meas,i}$$

The estimator presented in this work is also linear. Now let us fix a certain ray path. We first require (like in kriging [7], [8], [11]) that the estimator be unbiased i.e. the expectation of the estimated value is equal to the expectation of the real value:

$$E\left(\hat{I}_{unknown}\right) = E\left(I_{unknown}\right)$$

If we introduce in this equation the assumed ionospheric model (see the previous section) we end up with the linear constraint on the coefficients:

$$\sum_{k=1}^{p} \varphi_{k,unknown} \cdot ob_{k,unknown} = \sum_{i=1}^{n} \lambda_i \cdot \left(\sum_{k=1}^{p} \varphi_k \cdot ob_{k,i}\right)$$

The next step is the minimization of the estimation variance (subject to the linear constraint above):

$$E\left(\hat{I}_{unknown} - I_{unknown}\right)^2 = \sum_{i,j} \lambda_i \lambda_j \left(\operatorname{cov}\left(I_i, I_j\right) + M_{i,j}\right)$$

$$-2\sum_{i=1}^{n} \operatorname{cov}\left(I_i, I_{unknown}\right) + \operatorname{cov}\left(I_{unknown}, I_{unknown}\right)$$

As in kriging, the estimation variance is a quadratic form of the coefficients, and the form of the solution is the same [8], [12]:

$$\lambda = \left(W - WG\left(G^T WG\right)^{-1} G^T W\right)c + WG\left(G^T WG\right)^{-1} X_{unknown}$$

where W is the inverse of the covariance of the measurements (coming both from the ionosphere and the measurement noise):

$$W = \left(\mathrm{cov}\left(I_i, I_j\right) + M\right)^{-1}$$

$c$ is an $n$ by 1 vector defined by:

$$c_i = \mathrm{cov}\left(I_{unknown}, I_i\right)$$

$G$ is an $n$ by 1 vector defined by:

$$G_i = \sum_{k=1}^{p} \varphi_k \cdot ob_{k,i}$$

and finally:

$$X_{unknown} = \sum_{k=1}^{p} \varphi_k \cdot ob_{k,unknown}$$

The multiple layers are only used to compute the covariance between the measurements (we do not attempt to estimate each layer). As with kriging, the error bound is derived from the estimation variance [7], [8]. The estimation variance is given by the equation:

$$\sigma_{est}^2 = \sum_{i,j} \lambda_i \lambda_j \left(\mathrm{cov}\left(I_i, I_j\right) + M_{i,j}\right)$$
$$-2\sum_{i=1}^{n} \mathrm{cov}\left(I_i, I_{unknown}\right) + \mathrm{cov}\left(I_{unknown}, I_{unknown}\right)$$

$\sigma^2_{est}$ depends on the assumed average density profile, the assumed covariance dependence on each of the layers, and the geometry of the surrounding measurements. This method can be interpreted as a generalization of ordinary kriging to a multilayer setting. For this reason we will designate it in this paper by *extended kriging*.

## RESULTS

In this section we evaluate the performance of extended kriging by computing the difference between the true delay and the estimated delay, and comparing it to the estimated error bound. We will compare this algorithm to two others: the planar fit used in the current WAAS algorithm [1] and a proposed improvement based on kriging [7], [11]. The algorithm was evaluated using real data gathered at dual frequency receivers over the United States (WAAS network) and Brazil (a selection of GIS stations). The WAAS data is the so-called supertruth data [6] and the Brazil data has been post-processed at JPL [4]. In both cases the tracks have been carrier smoothed and the satellite and receiver biases have been mostly removed. As a result, we have a low noise data set of slant GPS ionospheric delays. The data sets correspond to April 6, 2000 (severe storm), September 7, 2002 (moderate storm) and July 2, 2000 (quiet day) for the US and February 19 and 21, 2002 for Brazil. The data was decimated down to 500 seconds for the US and down to 150 seconds for Brazil. For the US, only the measurements taken from CONUS (Conterminous US) were tested. Figure 1 shows the location of the Brazilian reference stations.

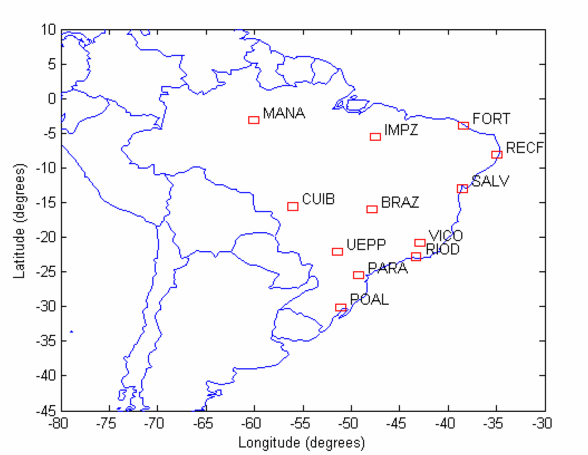


***Figure 1.*** *Reference station network over Brazil*

The method used to evaluate the algorithms is cross-validation: for each measurement from the data set, we compute the delay and the error bound using the remaining measurements. Because the method presented here relies on neighboring ray paths, we also excluded all of the measurements belonging to the same station. As with the current WAAS algorithm, past measurements are not used.

A new algorithm should not have more requirements for estimation (in number of measurements, for example) than the current algorithms: every time the current algorithm provides an estimate, the new algorithm has to provide one too. For each delay to be estimated, the selection of measurements to be used for the estimation was the same for the three algorithms: all measurements with IPPs (at 350 km height) within 1200 km of the ray path IPP were selected (excluding, as mentioned before, the ones taken at the same reference station). Also, a minimum of 10 points was required for estimation.

The results summarizing the accuracy of each of the algorithms for each day are presented in Tables 1 and 2. In order to compare the three algorithms we computed the corresponding vertical ionospheric delay for extended kriging. For each day and algorithm we tabulated the standard deviation of the error (top) and the maximum absolute error. These results need to be read with caution: some test measurements are too far from any measurement to be estimated correctly with any algorithm. Also, the data have been decimated, so some maximum error values could have been missed.

| | July 2, 2000 | | Sept. 7, 2002 | | Apr. 6, 2000 | |
|---|---|---|---|---|---|---|
| | rms | max | rms | max | rms | max |
| Planar | .21 | 1.7 | .55 | 5.4 | 1.68 | 10.7 |
| Kriging | .18 | 1.5 | .41 | 3.3 | 1.44 | 10.4 |
| Extended Kriging | .17 | 1.5 | .33 | 3.4 | .86 | 9.4 |

***Table 1.*** *Standard deviation of the error and maximum absolute error in meters in CONUS*

| | Feb. 19, 2002 | | Feb. 21, 2002 | |
|---|---|---|---|---|
| | rms | max | rms | max |
| Planar | 1.05 | 7.6 | 1.60 | 10.5 |
| Kriging | .85 | 5.7 | 1.13 | 8.5 |
| Extended Kriging | .64 | 5.1 | .90 | 8.0 |

***Table 2.*** *Standard deviation of the error and maximum absolute error in meters in Brazil*

The results corresponding to the new algorithm are always better than for the planar fit and kriging (and kriging is always better than the planar fit). The residuals are reduced by almost 50% over Brazil and on April 6 over the US. The maximum errors are not as dramatically reduced, but this is due to the edge location of some of the stations. For evidence of this, we show in Table 3 the results by reference station over Brazil for February 19.

| Station | Planar | | Kriging | | Extended Kriging | |
|---|---|---|---|---|---|---|
| | rms | max | rms | max | rms | max |
| BRAZ | 1.15 | 4.68 | .94 | 4.68 | .63 | 4.48 |
| CUIB | .92 | 4.01 | .82 | 3.82 | .69 | 3.10 |
| FORT | .99 | 4.65 | .87 | 4.18 | .84 | 5.10 |
| IMPZ | .97 | 4.06 | .92 | 3.52 | .85 | 4.22 |
| MANA | .90 | 3.27 | .76 | 2.38 | .68 | 1.70 |
| PARA | .96 | 5.94 | .66 | 4.96 | .45 | 5.03 |
| POAL | .93 | .4.55 | .75 | 4.26 | .60 | 4.01 |
| RECF | .96 | 7.15 | .86 | 5.72 | .68 | 4.81 |
| RIOD | .99 | 5.16 | .60 | 3.59 | .42 | 2.48 |
| SALV | 1.19 | 6.50 | 1.03 | 5.20 | .72 | 4.11 |
| UEPP | 1.06 | 6.02 | .88 | 4.81 | .62 | 3.88 |
| VICO | 1.05 | 7.64 | .77 | 5.09 | .50 | 3.44 |

***Table 3.*** *Standard deviation of the error and maximum absolute error in meters for each station in Brazil on February 19,2002.*

If we exclude Fortaleza (FORT) and Imperatriz (IMPZ) where the maximum error is slightly larger, both the standard deviation and the maximum error are dramatically decreased (up to 50%), especially in the well covered stations. The residuals as a function of time are shown in the Appendix.

The second part of the evaluation consists on comparing the actual error to the computed error bound. (Here the error bound will designate the standard deviation of the expected error). The error bound is the product of the square root of the estimation variance and an inflation factor $R_{irreg}$, which is a function of the chi-square statistic. The determination of this inflation factor is exposed in [8]. Here it suffices to say that it is meant to inflate the error bound according to the ionospheric behavior.

$$R_{irreg}^2 = \alpha_n I_{meas}{}^T \left( W - WG^T \left( G^T WG \right)^{-1} GW \right) I_{meas}$$

In this equation, the factor $\alpha_n$ is a constant function of the number of measurements and it is given in the Appendix. $I_{meas}$ is the vector of measurements used of estimation. We have:

$$\text{error bound} = R_{irreg} \sigma_{est}$$

Once we have the error bound we form the ratio:

$$\text{normalized residual} = \frac{\text{estimated vertical delay - computed vertical delay}}{\text{error bound}}$$

The result for February 19, 2002 over Brazil is shown in a histogram in Figure 2:

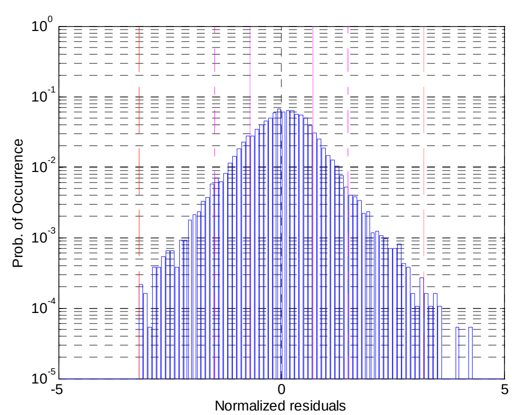


***Figure 2.*** *Normalized residuals for February 19, 2002*

These residuals where obtained with the error bounds shown in Figure 3.

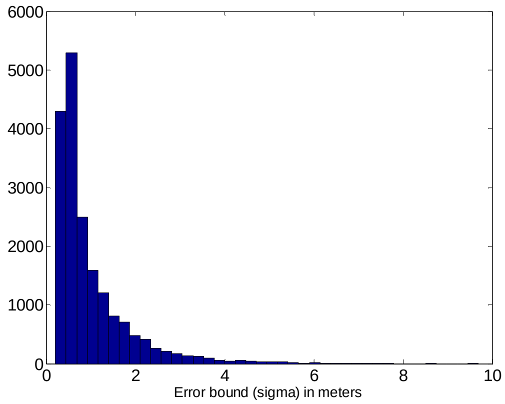


***Figure 3.*** *Error bound distribution for February 19, 2002*

Except for some outliers (due to the edge of coverage location of some of the stations where the ionosphere is more disturbed than in the locations where there are available measurements), the error bounds behave correctly. These results, although preliminary, show that it is possible to compute an error bound with this algorithm.

## CONCLUSION

Extended kriging reduces the estimation errors between 30% and 50% compared to a planar fit on the thin shell and between 15% and 30% compared to kriging. This result suggests that many of the features of the ionosphere as projected on the thin shell seen during disturbed conditions are due to limitations in the thin shell model itself, and that there is a way of reducing the ionospheric estimation errors even during ionospheric storms and in low latitudes, in particular in well covered locations. However, because the current SBAS message relies on the thin shell model, this technique cannot be applied in the current standards.

The next step will consist on checking whether the benefit of this method holds over the course of at least five minutes (five minute is the update rate of ionospheric information in WAAS) and on optimizing these results by finding more appropriate vertical profile functions. If the results are consistently better than the thin shell approach, it will be worth studying the minimum bandwidth requirements. If they are not achievable, it might still be possible to take some advantage of these results within the current algorithm by reducing our threat models [2].

The results presented so far strongly indicate that there is a real benefit of extending kriging to a multilayer setting. Furthermore, this technique has demonstrated that it does mitigate the limitations of the thin shell model while not adopting the problems of tomography.

## APPENDIX

*Additional results*

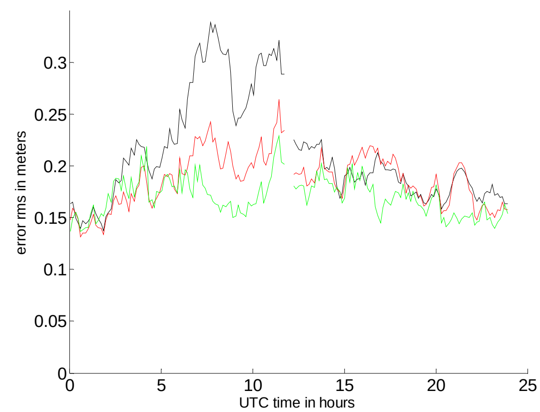


***Figure 4.*** *Standard deviation of the errors as a function of time on July 2, 2000 in the US*

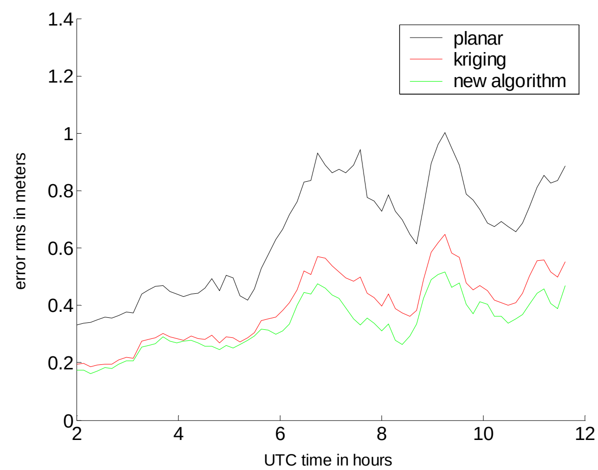


***Figure 5.*** *Standard deviation of the errors as a function of time on September 7, 2002 in the US*

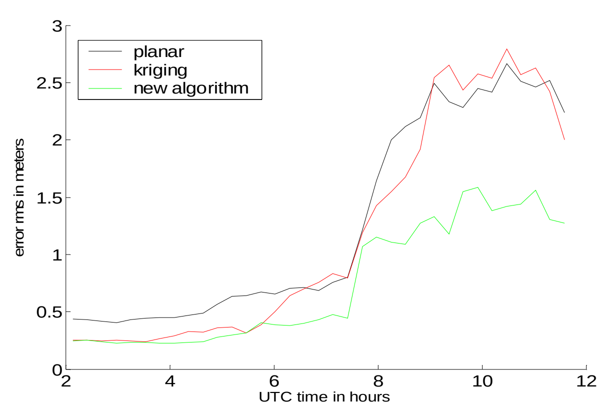


***Figure 6.*** *Standard deviation of the errors as a function of time on April 6, 2000 in the US*

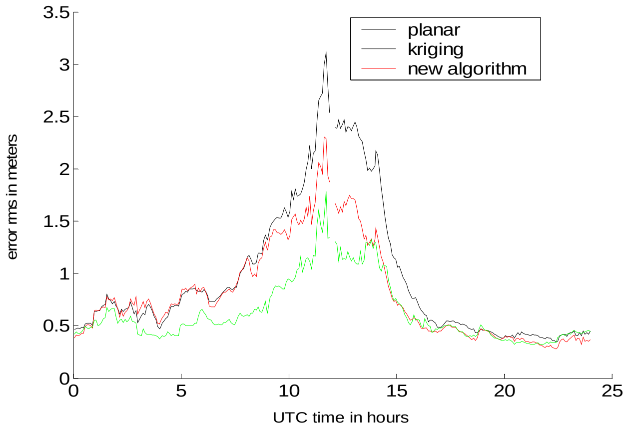


***Figure 7.*** *Standard deviation of the errors as a function of time on February 19, 2002 in Brazil*

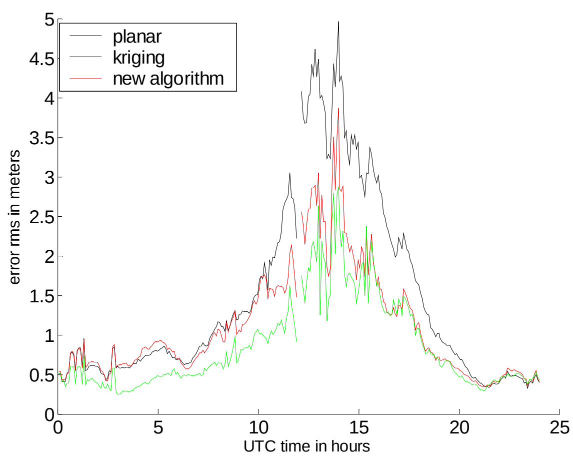


***Figure 8.*** *Standard deviation of the errors as a function of time on February 21, 2002 in Brazil*

*Table of* $\alpha_n$

| $n$ | $\alpha_n$ | $n$ | $\alpha_n$ | $n$ | $\alpha_n$ | $n$ | $\alpha_n$ |
|---|---|---|---|---|---|---|---|
| 10 | 1.208 | 19 | 0.164 | 28 | 0.075 | 37 | 0.047 |
| 11 | 0.824 | 20 | 0.146 | 29 | 0.070 | 38 | 0.045 |
| 12 | 0.600 | 21 | 0.131 | 30 | 0.066 | 39 | 0.043 |
| 13 | 0.459 | 22 | 0.119 | 31 | 0.062 | 40 | 0.041 |
| 14 | 0.365 | 23 | 0.109 | 32 | 0.059 | 41 | 0.040 |
| 15 | 0.299 | 24 | 0.100 | 33 | 0.056 | 42 | 0.038 |
| 16 | 0.251 | 25 | 0.092 | 34 | 0.053 | 43 | 0.037 |
| 17 | 0.214 | 26 | 0.086 | 35 | 0.051 | 44 | 0.036 |
| 18 | 0.186 | 27 | 0.080 | 36 | 0.049 | 45 | 0.035 |

***Table 4.*** *Factor α multiplying the chi-square statistic.*


## ACKNOWLEDGEMENTS

This work was sponsored by the FAA GPS product team (AND-730). The authors would also like to thank the WAAS team at Raytheon, for providing the supertruth data, and Dr. Attila Komjathy, for providing the Brazilian post-processed data.


## REFERENCES


[1] T. Walter *et al.* "Robust Detection of Ionospheric Irregularities," *Navigation, Journal of the U.S. Institute of Navigation*, Vol. 48, No. 2, Summer 2001.

[2] L. Sparks *et al.* "The WAAS Ionospheric Threat Model," *Proceedings of the Beacon Satellite Symposium*, Boston, MA, 2001.

[3] T. McHugh *et al.* "WAAS Observed Performance During 60 Day Test," *Proceedings of the Institute of Navigation National Technical Meeting*, Anaheim, 2003.

[4] A. L. Komjathy, L. Sparks, T. Mannucci, X. Pi. "Assessment of WAAS Ionospheric Correction Algorithms in the South American Region," *Proceedings of the Institute of Navigation GPS-02*. Portland, OR, 2002.

[5] RTCA Special Committee 159, *Minimum Operational Performance Standards for Airborne Equipment Using Global Positioning System/ Wide Area Augmentation System*, RTCA/DO-229C, November 2001.

[6] A. Hansen *et al.* "Ionospheric Correlation Analysis for WAAS: Quiet and Stormy," *Proceedings of the Institute of Navigation GPS-00*, 2000.

[7] J. Blanch. "An Ionospheric Estimation Algorithm for WAAS Based on Kriging," *Proceedings of the Institute of Navigation GPS-02*. Portland, OR, 2002.

[8] J. Blanch. *Using Kriging to bound Satellite Ranging Errors Due to the Ionosphere.* PhD thesis, Stanford University, 2003.

[9] A. Hansen. *Tomographic Estimation of the Ionosphere Using Terrestrial GPS Sensors*. PhD thesis, Stanford University, 2002.

[10] R. Lejeune, M.B. El-Arini. "Performance of a Tomographic Approach to SBAS Ionospheric Estimation in the Equatorial Region," *Proceedings of the Institute of Navigation National Technical Meeting*, San Diego, CA, 2004.

[11] R. Webster, M. Oliver. *Geostatistics for Environmental Scientists*. John Wiley and Sons, New York, 2001.

[12] J. Blanch, T. Walter, P. Enge. "Adapting Kriging to the WAAS MOPS Ionospheric Grid," *Proceedings of the Institute of Navigation National Technical Meeting*, Anaheim, 2003.